

Hydrogenic-donor impurity states in coupled quantum disks in the presence of a magnetic field

Li-Zhe Liu and Jian-Jun Liu^{a)}

College of Physical Science and Information Engineering, Hebei Normal University, Shijiazhuang, Hebei 050016, People's Republic of China

(Received 29 April 2007; accepted 19 June 2007; published online 8 August 2007)

We report the binding energies of a hydrogenic-donor impurity in a cylindrically symmetric GaAs/Ga_{1-x}Al_xAs-coupled quantum disk in the presence of a uniform magnetic field for different disk and barrier thicknesses, disk radii, and donor ion positions within the disk. The magnetic field is assumed to be applied parallel to the disk axis. The calculations were performed using a variational procedure for finite-confinement potentials within the effective-mass approximation. The calculated results show that the binding energy is dependent on the interplay of the spatial confinement and magnetic-field confinement: A high magnetic field significantly enhances the binding energy in the case of weak spatial confinement. The binding energy of a hydrogenic-donor impurity in two coupled quantum disks is found to be smaller than that in a corresponding single quantum disk, due to the coupling effect between the disks. In the limits of coupled quantum wells, the results we obtain are in good agreement with those previously obtained for the case in which the donor ion is located at the center of the quantum disk. © 2007 American Institute of Physics. [DOI: 10.1063/1.2764232]

I. INTRODUCTION

With the development of molecular-beam epitaxy and metal-organic chemical-vapor deposition,¹⁻⁶ we can now precisely control the distance between two material layers of particular compositions and doping profiles to within a few angstroms. If the layers are thin enough, the coupling effects between adjacent quantum disks become significant and can result in the formation of a superlattice. The effects of quantum confinement on the electronic and optical properties then become more obvious. An external perturbation of a system, such as the application of a magnetic field, is a powerful tool for studying the properties of matter, and it leads to many investigations in semiconductor systems. The optical properties associated with a shallow-donor impurity in coupled quantum disks under a magnetic field are of interest for their relevance to the application of a magnetic field perpendicular to the semiconductor layers.

Coupled pairs of quantum dots, which could be referred to as artificial molecules, have been the subject of much research.⁷⁻²¹ Understanding the physics of impurity states in quantum wires,²²⁻²⁴ double quantum wells,²⁵⁻³⁰ and quantum dots³¹⁻⁴³ is also an important problem in semiconductor physics. Several factors affect the binding energies of a shallow-donor impurity⁴⁴ in coupled quantum disks, including the applied magnetic field, the sizes of the quantum disks, the barrier thickness, and the position of the donor ion. The interplay of the spatial confinement and magnetic-field confinement of the electron and the donor ion in the coupled quantum disks leads to complex behavior of the binding energy. The binding energies in such a system are expected to be smaller than those in a single quantum disk due to the coupling effect between the two disks.

Extensive theoretical work on the coupling effect has been reported.⁴⁵⁻⁵⁰ Troiani and Hohenester carried out theoretical investigations of correlated electron-hole states in vertically coupled quantum dots.⁵¹ Excitonic trions in quantum dots with a Gaussian confinement potential were studied by the variational method.⁵² The ground- and excited-state properties of vertically coupled quantum dots were studied by exact diagonalization.⁵³ Ugajin calculated the optical transition coefficient of two electrons confined in a square-well quantum dot in the presence of a magnetic field.⁵⁴ The coherent manipulation of a double quantum dot system by an external driving field was analyzed using a controlled rotation method.⁵⁵ Li *et al.* studied the binding energies of a hydrogenic-donor impurity in cylindrical quantum disks using a variational approach.⁵⁶ The calculated results show stronger confinement and larger binding energies for a hydrogenic-donor impurity in cylindrical disks than in corresponding quantum wires and quantum wells. The binding energy increases as the radius and thickness of the quantum disk decrease, while a high magnetic field markedly enhances the binding energy in the case of weak spatial confinement, especially for larger disk radii. However, there has been no report of the calculation of the binding energy of a hydrogenic-donor impurity in a double cylindrical quantum disk in the presence of a uniform magnetic field. The study of the behaviors of binding energies and electron probability of such systems under applied magnetic fields will lead to a better understanding of the electronic and optical properties of low-dimensional semiconductor systems.

In this paper we report the calculation of the binding energy of a hydrogenic-donor impurity in coupled quantum disks in the presence of a magnetic field along the disk axis for different positions of the donor ion under the condition of electron effective-mass mismatch. The Hamiltonian of our

^{a)}Electronic mail: liujj@mail.hebtu.edu.cn

system, including the kinetic energy term, the spatial confinement term, and the term of the Coulomb interaction between the electron and donor ion, is too complex to be solved directly. Thus, a variational technique is applied to obtain numerical results. Following the theory of Li *et al.*,⁵⁶ we obtain a trial wave function that includes the appropriate confining confluent hypergeometric functions term, a function term from the z -direction spatial confinement, and a hydrogenic term. This paper is organized as follows. In Sec. II, the theoretical framework is given for known applied magnetic-field and spatial-confinement potentials. We also present explicit formulas for calculating the binding energy. In Sec. III, we present and discuss our results. Finally, our conclusions are presented in Sec. IV.

II. THEORETICAL FRAMEWORK

Within the effective-mass approximation, the Hamiltonian for a shallow-donor impurity in cylindrically symmetric coupled quantum disks surrounded by a finite-potential barrier, in the presence of a magnetic field parallel to the disks axis, is given by

$$H = \left(\vec{p} + \frac{e}{c} \vec{A} \right)^2 / 2m_{b,d}^* - \frac{e^2}{\epsilon_{d,b} |\vec{r} - \vec{r}_0|} + V(\rho, \phi, z), \quad (1)$$

where $|\vec{r} - \vec{r}_0| = [\rho^2 + \rho_0^2 - 2\rho\rho_0 \cos[\phi - \phi_0] + (z - z_0)^2]^{1/2}$ is the distance between the electron and the donor ion, $\vec{A}(\vec{r})$ is the magnetic-field vector potential, \vec{r}_0 is the position of the donor ion, and the subscripts d and b stand for the quantum disk and barrier-layer materials, respectively. $m_{b,d}^*$ and $\epsilon_{b,d}$ are the conduction effective masses and the dielectric constants of the barrier and the quantum disk layer materials, respectively. The barrier effective mass, dielectric constant, and potential barrier height depend on the aluminum concentration (x), $m_b^* = m_d^* + 0.083xm_0$, $\epsilon_b = 13.13 \times (1-x) + 10.1x$,⁵⁷ and the finite-potential barrier height $V_i = Q_e(1.36x$

$+ 0.22x^2)$ (eV),⁵⁸ where $Q_e = 0.6$ and m_0 is the free-electron mass.

The dielectric constant mismatch between ϵ_b and ϵ_d affects the binding energy mainly for small sizes of the quantum disks and high aluminum concentrations.⁵⁹ Strictly speaking, the image potential in coupled quantum disks cannot be neglected when considering electronic and impurity states, especially when the sizes of the disks are small. However, in our calculations the structures of the coupled quantum disks are generally large and the aluminum concentration is taken as $x = 0.3$. In addition, since we focus on the effect of the magnetic field on the binding energy, dielectric constant mismatch between the disk and barrier can be neglected. This means that in our calculations $\epsilon_b = \epsilon_d$. The $V(\rho, \phi, z)$ is the spatial confinement that confines the electron in the quantum disk, and is given by

$$V(\rho, \phi, z) = \begin{cases} 0, & \text{for } 0 \leq \rho \leq R \text{ and } L_c > |z| > L_b/2, \\ V_0, & \text{for } \rho > R, \\ V_i, & \text{for } 0 \leq \rho \leq R, |z| \leq L_b/2 \text{ and } |z| \geq L_c, \end{cases} \quad (2)$$

where $L_c = L_b/2 + L_d$ and $V_0 = V_i$ (the aluminum concentration for the barrier materials outside the disk is assumed to be $x = 0.4$).

The quantities L_d , L_b , V_i , and R denote the thickness of the quantum disk, the thickness of the barrier, the barrier height, and the radius of the coupled quantum disks, respectively.

It is observed that the trial wave function is divided into two parts here in order to obtain the converging solutions for $R = \infty$ and $R = 0$. Following Li *et al.*,⁵⁶ we obtain a trial wave function that includes confluent hypergeometric function terms ${}_1F_1(-a_{01}, 1; \xi)$ and $U(-a'_{01}, 1; \xi)$ from radial confinement, an $f(z)$ term due to the z -direction confinement, and a hydrogenic term. The trial wave function is therefore chosen as

$$\psi(r) = \begin{cases} N {}_1F_1(-a_{01}, 1; \xi) f(z) \exp\left[-\frac{\xi}{2} - \lambda(\rho^2 + (z - z_0)^2)^{1/2}\right], & \text{for } 0 \leq \rho \leq R, \\ N \frac{{}_1F_1(-a_{01}, 1; \xi_R)}{U(-a'_{01}, 1; \xi_R)} U(-a'_{01}, 1; \xi) f(z) \exp\left[-\frac{\xi}{2} - \lambda(\rho^2 + (z - z_0)^2)^{1/2}\right], & \text{for } \rho > R, \end{cases} \quad (3)$$

where $\alpha_c = (\hbar c / eB)^{1/2}$ is the cyclotron radius, z_0 gives the donor ion position along the z -direction, $\xi = \rho^2 / 2\alpha_c^2$, $\xi_R = R^2 / 2\alpha_c^2$, N is the normalization constant, and λ is a variational parameter. The terms ${}_1F_1(-a_{01}, 1; \xi)$ and $U(-a'_{01}, 1; \xi)$ are the confluent hypergeometric functions (Kummer functions), which are obtained by solving the Schrodinger equation for a cylindrical double quantum disk, in the presence of a magnetic field along the disk axis. Equation (3) satisfies the boundary condition, while a_{01} and a'_{01} are the ground-state eigenvalues of the electron inside and outside the coupled quantum disks, respectively, being calculated numerically by using the expressions

$$\frac{1}{m_d^*} \left. \frac{\partial \exp(-\xi/2) {}_1F_1(-a_{01}, 1; \xi)}{\partial \rho} \right|_{\rho=R} = \frac{1}{m_b^*} \left. \frac{{}_1F_1(-a_{01}, 1; \xi_R) \partial \exp(-\xi/2)}{U(-a'_{01}, 1; \xi_R) \partial \rho} U(-a'_{01}, 1; \xi) \right|_{\rho=R} \quad (4)$$

and

$$\hbar\omega_d\left(a_{01} + \frac{1}{2}\right) - \hbar\omega_b\left(a'_{01} + \frac{1}{2}\right) = V_0. \quad (5)$$

In addition, $f(z)$ is the eigenfunction along the z direction,⁶⁰

$$f(z) = \begin{cases} +A \exp[\beta(z + L_c)], & \text{for } z \leq -L_c, \\ -B \sin[\eta(z + L_b/2)] + C \cos[\eta(z + L_b/2)], & \text{for } -L_c < z < -L_b/2, \\ +\cosh(\beta z), & \text{for } |z| \leq L_b/2, \\ +B \sin[\eta(z - L_b/2)] + C \cos[\eta(z - L_b/2)], & \text{for } L_b/2 < z < L_c, \\ +A \exp[-\beta(z - L_c)], & \text{for } z \geq L_c, \end{cases} \quad (6)$$

where

$$\eta = \left[\frac{2m_d^* E_z}{\hbar^2} \right]^{1/2}, \quad \beta = \left\{ \frac{2m_b^*}{\hbar^2} [v_i - E_z] \right\}^{1/2}. \quad (7)$$

The coefficients A , B , and C are also obtained from the boundary conditions of the eigenfunction $f(z)$ at the interfaces. The corresponding eigenvalue associated with $f(z)$, E_z , may be obtained as the first root of the transcendental equation

$$2 \cos(\eta L_d) + \left(\mu - \frac{1}{\mu} \right) \sin(\eta L_d) - \left(\mu + \frac{1}{\mu} \right) \sin(\eta L_d) \times \exp(-\beta L_b) = 0, \quad (8)$$

where $\mu = m_d^* \beta / m_b^* \eta$.

The expectation value of the Hamiltonian H is given by

$$E = \frac{\int \psi^* H \psi d\tau}{\int \psi^* \psi d\tau}. \quad (9)$$

In order to obtain a lower bound to the ground state of the system, we search for the minimum of E with respect to λ by using a variational method. In order to calculate this, we normalize the expression for the binding energy in units of meV, and define the angstrom as the unit of length. The explicit formula for calculating the binding energy is

$$E_b(R, B, L_b, L_d) = \frac{\hbar^2}{2m_{b,d}^*} [\lambda^2 AA - 2\lambda BB - 2\lambda CC - 2\lambda DD] / AA + \frac{e^2}{\epsilon_{b,d}} (BB/AA), \quad (10)$$

where

$$AA = \int_0^R d\rho_1 F_1^2(-a_{01}, 1; \xi) \exp(-\xi - 2\lambda[\rho^2 + (z - z_0)^2]^{1/2}) \rho \times \int_{-\infty}^{+\infty} f^2(z) dz + \frac{1}{U^2(-a'_{01}, 1; \xi_R)} \int_R^{+\infty} d\rho U^2(-a'_{01}, 1; \xi) \exp(-\xi - 2\lambda[\rho^2 + (z - z_0)^2]^{1/2}) \rho \int_{-\infty}^{+\infty} f^2(z) dz,$$

$$BB = \int_0^R d\rho_1 F_1^2(-a_{01}, 1; \xi) \exp(-\xi - 2\lambda[\rho^2 + (z - z_0)^2]^{1/2}) \rho \times \int_{-\infty}^{+\infty} f^2(z) / [\rho^2 + (z - z_0)^2]^{1/2} dz + \frac{1}{U^2(-a'_{01}, 1; \xi_R)} \int_R^{+\infty} d\rho U^2(-a'_{01}, 1; \xi) \exp(-\xi - 2\lambda[\rho^2 + (z - z_0)^2]^{1/2}) \rho \times \int_{-\infty}^{+\infty} f^2(z) / [\rho^2 + (z - z_0)^2]^{1/2} dz,$$

$$CC = \int_0^R d\rho_1 F_1(-a_{01}, 1; \xi) \exp\left(-\frac{\xi}{2}\right) \frac{\partial}{\partial \rho} \left[F_1(-a_{01}, 1; \xi) \times \exp\left(-\frac{\xi}{2}\right) \right] \exp(-2\lambda[\rho^2 + (z - z_0)^2]^{1/2}) \rho^2 \times \int_{-\infty}^{+\infty} f^2(z) / [\rho^2 + (z - z_0)^2]^{1/2} dz + \frac{1}{U^2(-a'_{01}, 1; \xi_R)} \int_R^{+\infty} d\rho U(-a'_{01}, 1; \xi) \exp\left(-\frac{\xi}{2}\right) \frac{\partial}{\partial \rho} \left[U(-a'_{01}, 1; \xi) \times \exp\left(-\frac{\xi}{2}\right) \right] \exp(-2\lambda[\rho^2 + (z - z_0)^2]^{1/2}) \rho^2 \times \int_{-\infty}^{+\infty} f^2(z) / [\rho^2 + (z - z_0)^2]^{1/2} dz,$$

$$DD = \int_0^R d\rho_1 F_1^2(-a_{01}, 1; \xi) \exp(-\xi - 2\lambda[\rho^2 + (z - z_0)^2]^{1/2}) \rho \times \int_{-\infty}^{+\infty} f(z) f'(z) / [\rho^2 + (z - z_0)^2]^{1/2} dz + \frac{1}{U^2(-a'_{01}, 1; \xi_R)} \int_R^{+\infty} d\rho U^2(-a'_{01}, 1; \xi) \exp(-\xi - 2\lambda[\rho^2 + (z - z_0)^2]^{1/2}) \rho \times \int_{-\infty}^{+\infty} f(z) f'(z) / [\rho^2 + (z - z_0)^2]^{1/2} dz.$$

The above integrations are performed numerically.

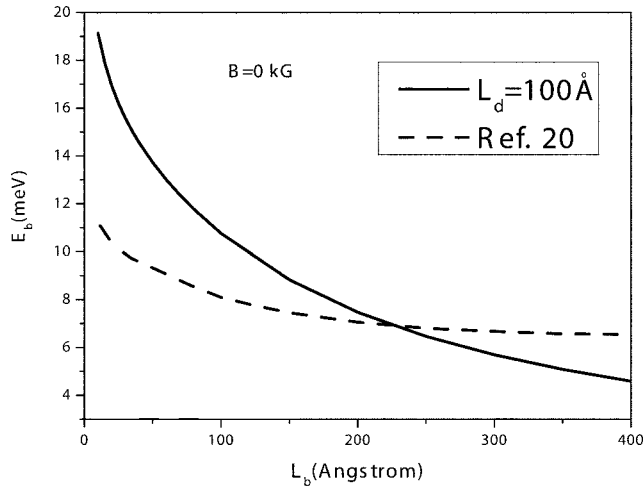


FIG. 1. Shallow-donor binding energies as functions of the barrier thickness in coupled quantum disks with a disk thickness of 100 Å and a disk radius of 100 Å in the absence of a magnetic field for the donor ion located at the center of the barrier. The solid curve is the results of the coupled quantum disks; the dashed curve is the result in Ref. 20.

III. RESULTS AND DISCUSSION

We have calculated the ground-state binding energy for different positions of the donor ion, in the presence of a uniform magnetic field applied along the z direction. The values of the physical parameters for GaAs used in our calculation are $m_d^* = 0.067m_0$ and $\epsilon_d = 12.5$.

In Fig. 1 we compare the binding energy of a donor ion as a function of barrier thickness in symmetrical coupled quantum disks for $L_d = 100$ Å and $R = 100$ Å with the result for a donor ion located at the center of the barrier in the absence of a magnetic field. The behavior of the binding energy as a function of the barrier thickness for coupled quantum disks is similar to that of Ref. 20. However, our results are different from those of Wang,²⁰ because the potentials of the two structures are not completely identical.

The ground-state theoretical results of the binding energy with the zero-magnetic-field limit, for a barrier thickness of 100 Å, are compared in Fig. 2 with the corresponding results of Thoai,⁶¹ as functions of the disk thickness and well thickness for the donor ion positions at the center of the disk and well. Due to the large values of R considered here, the structure of the coupled quantum disks is practically at the limiting case of the double quantum wells. It is exciting that the results of the coupled quantum disks are in quite good agreement with those of Ref. 61.

In Fig. 3 we present results for the binding energy as a function of the disk radius and for several values of the applied magnetic field when the donor ion is located at the center of the disk. As the disk radius decreases, the binding energy increases sharply at the beginning of the curves until a maximum value is obtained, and then it begins to drop quickly. This is due to the fact that the electron wave function is compressed into a small disk size by the finite-potential barrier for a small disk radius, and the leakage of the wave function into the barrier region becomes stronger, thus leading to a decrease of the binding energy. It is exciting to note that the positions at which the maximum value occurs

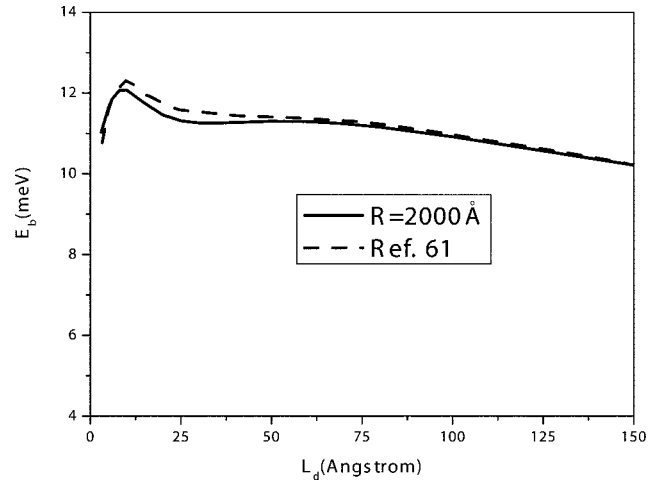


FIG. 2. Comparison of results for the binding energy of a hydrogenic-donor impurity in the coupled quantum disks for $R = 2000$ Å, $L_b = 100$ Å, and $B = 0$ kG with those of the double quantum well in Ref. 61. The donor ion is located at the center of the quantum disk.

for all curves are independent of the values of the applied magnetic field. This phenomenon stems from the complicated interplay of the spatial confinement and the Coulomb interaction, and the magnetic-field confinement for the small disk size. It is well known that the wave function can be compressed by the magnetic field, thus leading to a higher binding energy for large disk radius, and the effect of the magnetic field on the binding energy becomes more sensitive especially for the case of weak spatial confinement. In the infinitely large radius limit, our results converge asymptotically to those of the corresponding quantum-well structures because the effect of the radial confinement potential disappears, and the electron cyclotron radii are much smaller than the disk radii. In addition, binding energies in our work are smaller than those of a single quantum disk due to the coupling effect between the two quantum disks. It is interesting to note that our results are larger than that of a quantum wire

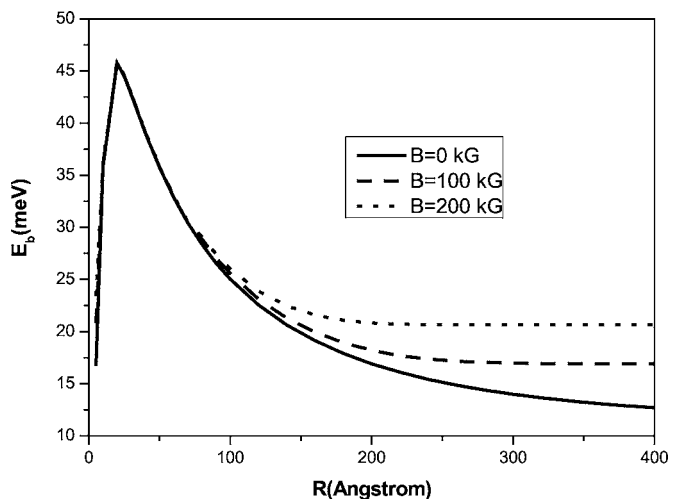


FIG. 3. Binding energy of a donor impurity as a function of the disk radius in symmetrical coupled quantum disks with $L_b = L_d = 100$ Å, for $B = 0$ kG, $B = 100$ kG, and $B = 200$ kG, for the case in which the donor ion is located at the disk center.

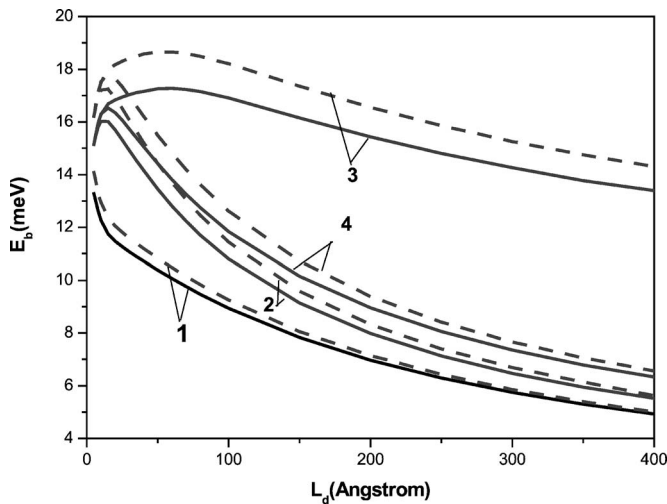


FIG. 4. Binding energy of a donor ion as a function of the thickness of the disks in cylindrically symmetric coupled quantum disks with $L_b=100$ Å and $R=200$ Å, for $B=0$ kG (solid lines) and $B=100$ kG (dashed lines). The labels 1, 2, 3, and 4 correspond to the donor ion at the barrier center, barrier edge, disk center, and disk edge, respectively.

in the presence of a magnetic field applied along the wire axis,⁵⁸ due to the effect of the confining potentials of the z direction.

In Fig. 4 we display the variation of the ground-state binding energy as a function of the disk thickness in cylindrically symmetric coupled quantum disks with $L_b=100$ Å and $R=200$ Å, when the donor ion is located at the barrier center, barrier edge, disk center, and disk edge. As a general feature, the binding energies increase as the disk thickness increases until they reach maximum values, and then they begin to diminish monotonically. The values of the binding energy, which depend on the complex interplay of the spatial confinement, Coulomb interaction, and the magnetic field confinement, are not the largest for the smallest disk sizes due to the contribution of the left disk. It is well known that the distance between the electron and the donor ion reaches its minimum value when the maximum value of the binding energy is obtained. Comparing curves “3” with the others, it is found that the binding energy is insensitive to the variation of disk thicknesses for large disk thickness when the donor ion is located at the center of the right disk. This can be explained by the fact that the electron is strongly confined into the right disk by the donor ion and has less freedom to penetrate into the second, since the effect of the left disk on the binding energy is relatively weak and the average distance between the electron and the donor ion remains almost constant. If the disk thickness is very large, the distribution of the electron cloud approaches that of a single quantum disk for the donor ion at the disk center. When the disk thickness goes to zero, we note that the binding energy approaches the bulk value characteristic of the barrier material for all the lines, as expected. With decreasing disk radius, the electron wave function is squeezed and begins to penetrate into the radial barrier region, which is equivalent to reducing the radial confinement. On the other hand, the effect of the radial confinement on the leakage of the wave function becomes inconspicuous for large disk radii. Due to the large

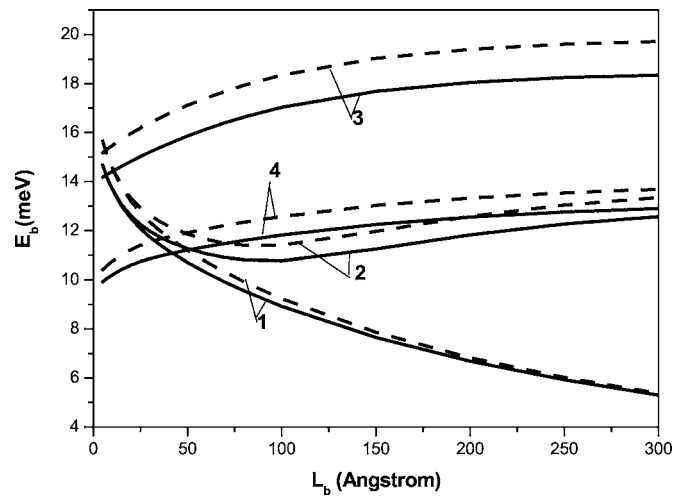


FIG. 5. Binding energy of a donor ion as a function of the barrier thickness in cylindrically symmetric coupled quantum disks with $L_d=100$ Å and $R=200$ Å for $B=0$ kG (solid lines) and $B=100$ kG (dashed lines). The labels 1, 2, 3, and 4 are the same as those in Fig. 4.

values of the disk radius ($R=200$ Å) considered here, the effect of leakage of the wave function on the binding energy becomes very weak while the influences of the Coulomb interaction and applied magnetic field on the binding energy are accordingly enhanced. These calculations show that the values of the disk thickness at which the binding energy reaches its maximum value are about the same positions for all values of the applied magnetic field. This is due to the fact that the portion of the wave function in cylindrically symmetric coupled quantum disks is determined primarily by the wave function including the z component, which is independent of the magnetic field. In addition, in the limit of infinitely large disk thickness values, it is interesting to note that the binding energy for the donor ion located at the disk center goes to the exact limit of the donor ion in a single quantum disk.

The binding energy of a donor ion as a function of the thickness of the central barrier for several donor ion positions and two values of the applied magnetic field along the disk axis are presented in Fig. 5. It is interesting that the pair of the two quantum disks becomes a single quantum disk of thickness 200 Å when the central barrier thickness approaches zero, since the central barrier disappears and the electron can occupy a larger free space. The two curves labeled “1” and “2” with solid lines (dashed lines) reach the same values of the binding energy for small barrier thickness ($L_b < 20$ Å). This can be understood by noting that the effect of the different positions of the donor ion on the binding energy becomes very weak when the donor ion is located at the barrier center and barrier edge. It is clear that for a large barrier thickness ($L_b > 200$ Å), the values of the binding energy converge to the results of a single quantum disk due to the weak coupling effect between the two quantum disks for the case in which the donor ion is at the disk center. The binding energy always decreases monotonically with increasing barrier thickness for the case of the donor ion at the barrier center. In addition, the effect of the applied magnetic field on the binding energy becomes weaker as the barrier

thickness increases, and thus the results of the solid and dashed lines reach the same values. In the infinitely large barrier thickness limit, the binding energy will go to zero because the wave function cannot easily penetrate into the barrier region and the distance between the donor ion and the electron becomes infinitely large, and thus the Coulomb interaction between the donor ion and the electron disappears. It is worth noting that for the curves labeled “2,” “3,” and “4,” the change in the binding energy is not sensitive to increases in the barrier thickness for $L_b > 200 \text{ \AA}$, and the effect of the left disk on the right disk can be neglected. This is due to the fact that the effect of the left disk on the binding energy is reduced by the increasing barrier thickness, and the binding energy of the coupled quantum disks will approach that of uncoupled quantum disks. When the donor ion is located at the barrier edge, it is observed that the binding energy diminishes until it reaches a minimum value, at which point it then increases gradually, and finally coincides with the curves labeled “4.” The merging of curves 2 and 4 is the limiting case of a single quantum disk for sufficiently large barrier thickness. In conclusion, the coupling effect between the two quantum disks on the binding energy gradually becomes weaker for all positions of the donor ion and two values of the applied magnetic field, when the barrier thickness is larger than 200 \AA . In this case, the barrier thickness is large enough to impede the wave function penetration into the other quantum disk, so the values of the binding energy will converge to the results of a corresponding single quantum disk and the distribution of the electron cloud becomes symmetric like that of a single quantum disk with a donor ion at the disk center.

Finally, we would like to mention that we have tested the accuracy of our variational approach by considering the case in which the applied magnetic field is zero and the potential barriers are infinite, using the trial wave function in Ref. 24. The variation in the binding energy thus obtained is within a few percent of that calculated using our variational wave function for small values of the magnetic field ($B < 0.148 \text{ kG}$).

IV. CONCLUSIONS

We have presented the binding energies of a hydrogenic-donor impurity in cylindrical coupled quantum disks for different disk and barrier thicknesses, disk radii, and positions of the donor ion in the presence of a uniform magnetic field along the disk axis by using a variational procedure within the effective-mass approximation.

By calculating the effect of the radial confinement on the binding energy for several values of the magnetic field, it is observed that the binding energy continues to increase as the disk radius decreases until it reaches a peak value for a certain disk radius, and then drops sharply, while under the magnetic-field conditions additional increases for the binding energy are observed, especially for larger disk radii. In addition, in the limiting case of a corresponding double quantum well, it is worth remarking that our results are in excellent agreement with those in Ref. 61.

Calculations of the binding energy as a function of the

disk thickness have also been carried out. It is found that the binding energy of the donor ion at the disk center is much larger than for the case of the other positions of the donor ion. For a given magnetic field, the change in the binding energy is not sensitive to the increasing disk thickness when the donor ion is located at the disk center. The reason is that the electron cloud is strongly confined into the right disk by the donor ion and the contribution of the left disk to the binding energy is reduced, and thus the wave function begins to diminish at the boundaries.

The coupling effect between the two disks becomes very weak for all positions of the donor ion when the barrier thickness is larger than 200 \AA , and the wave function no longer penetrates easily into the second quantum disk, thus leading to a higher binding energy. In the limit of infinitely large barrier thickness, we found that the binding energy converges to the values of the binding energy of the corresponding single quantum disk. In the limiting case of a corresponding double well, our results are in excellent agreement with those in Ref. 61.

ACKNOWLEDGMENTS

This work was partially financed by the National Natural Science Foundation of China (Grant No. 10674040), the Science and Technology Innovation Foundation of Hebei Province (Grant No. 06547006D-4), and the Natural Science Foundation of Hebei Province (Grant No. A2007000233).

- ¹M. B. Stern, H. C. Craighead, P. F. Liao, and P. M. Mankiewich, *Appl. Phys. Lett.* **45**, 410 (1984).
- ²K. Kash, A. Scherer, J. M. Worlock, H. G. Graighead, and M. C. Tamargo, *Appl. Phys. Lett.* **49**, 1043 (1986).
- ³Y. Kimura, M. Cao, Y. Shingai, K. Furuya, Y. Suematsu, K. G. Ravikumar, and S. Arai, *Jpn. J. Appl. Phys.*, Part 2 **26**, L255 (1987).
- ⁴R. Rossetti, R. Hull, J. M. Gibson, and L. E. Brus, *J. Chem. Phys.* **82**, 552 (1985).
- ⁵H. Temkin, G. J. Dolan, M. B. Panish, and S. N. G. Chu, *Appl. Phys. Lett.* **50**, 413 (1987).
- ⁶F. R. Waugh, *Phys. Rev. Lett.* **75**, 705 (1995); *Phys. Rev. B* **53**, 1413 (1996).
- ⁷G. Bryant, *Phys. Rev. B* **44**, 3064 (1991).
- ⁸L. M. Ruzin, V. Chandrasekhar, E. I. Levin, and L. I. Glazman, *Phys. Rev. B* **45**, 13469 (1992).
- ⁹F. R. Waugh, M. J. Berry, C. H. Crouch, C. H. Livermore, D. J. Mar, R. M. Westervelt, K. L. Campman, and A. C. Gossard, *Phys. Rev. B* **53**, 1413 (1996).
- ¹⁰L. W. Molenkamp, K. Flensberg, and M. Kemerink, *Phys. Rev. Lett.* **75**, 4282 (1995).
- ¹¹J. M. Golden and B. I. Halperin, *Phys. Rev. B* **53**, 3893 (1996).
- ¹²J. H. Oh, K. J. Chang, G. Ihm, and S. J. Lee, *Phys. Rev. B* **53**, R13264 (1996).
- ¹³T. H. Oosterkamp, L. P. Kouwenhoven, A. E. Koolen, N. C. vander Vaart, and C. J. P. M. Harmans, *Phys. Rev. Lett.* **78**, 1536 (1997).
- ¹⁴H. Imamura and P. Hawrylak, *Phys. Rev. B* **53**, 12613 (1996).
- ¹⁵J. J. Palacios and P. Hawrylak, *Phys. Rev. B* **51**, 1769 (1995).
- ¹⁶J. Hu, E. Dagotto, and A. H. MacDonald, *Phys. Rev. B* **54**, 8616 (1996).
- ¹⁷T. Chakraborty, V. Halonen, and P. Pietilainen, *Phys. Rev. B* **43**, 14289 (1991).
- ¹⁸D. G. Austing, T. Honda, and S. Tarucha, *Jpn. J. Appl. Phys.*, Part 1 **36**, 1667 (1997).
- ¹⁹J.-J. Liu, M. Shen, and S.-W. Wang, *J. Appl. Phys.* **101**, 073703 (2007).
- ²⁰X. F. Wang, *Phys. Lett. A* **364**, 66 (2007).
- ²¹J.-L. Liu, S.-S. Li, Z.-C. Niu, F.-H. Yang, and S.-L. Feng, *Superlattices Microstruct.* **33**, 29 (2003).
- ²²X.-T. An and J.-J. Liu, *J. Appl. Phys.* **99**, 123713 (2006).
- ²³A. L. A. Fanyao, F. Fonseca, and O. A. C. Nunes, *Phys. Rev. B* **54**, 16405 (1996).

- ²⁴W. J. Brown and H. N. Spector, J. Appl. Phys. **59**, 1179 (1986).
- ²⁵R. Ranganathan, B. D. McCombe, N. Nguyen, Y. Zhang, and M. L. Rustgi, Phys. Rev. B **44**, 1423 (1991).
- ²⁶N. Nguyen, R. Ranganathan, B. D. McCombe, and M. L. Rustgi, Phys. Rev. B **44**, 3344 (1991).
- ²⁷H. Chen and S. Zhou, Phys. Rev. B **36**, 9581 (1987).
- ²⁸N. Nguyen, R. Ranganathan, B. D. McCombe, and M. L. Rustgi, Phys. Rev. B **45**, 11166 (1992).
- ²⁹E. Reyes-Gomez, A. Matos-Abiague, C. A. Perdomo-Leiva, M. de Dios-Leyva, L. E. Oliveira, N. Nguyen, R. Ranganathan, B. D. McCombe, and M. L. Rustgi, Phys. Rev. B **61**, 13104 (2000).
- ³⁰S. Chaudhuri, Phys. Rev. B **28**, 4480 (1983).
- ³¹Y. P. Varshni, Superlattices Microstruct. **29**, 233 (2001).
- ³²C. Bose and C. K. Sarkar, Physica B (Amsterdam) **253**, 238 (1998).
- ³³V. L. Nguyen, M. Trinh Nguyen, and T. Dat Nguyen, Physica B (Amsterdam) **292**, 153 (2000).
- ³⁴C. Bose, Physica E (Amsterdam) **4**, 180 (1999).
- ³⁵Q. Chen, Y. Ren, Z. Jiao, and K. Wang, Phys. Lett. A **252**, 251 (1999).
- ³⁶C.-Y. Chen, P.-W. Jin, W.-S. Li, and D. L. Lin, Phys. Rev. B **56**, 14913 (1997).
- ³⁷J. L. Zhu, Phys. Rev. B **39**, 8780 (1989).
- ³⁸J. L. Zhu, J. J. Xiong, and B. L. Gu, Phys. Rev. B **41**, 6001 (1990).
- ³⁹G. T. Einevoll and Y. C. Chang, Phys. Rev. B **40**, 9683 (1989).
- ⁴⁰A. L. A. Fanyao, F. Fonseca, and O. A. C. Nunes, J. Appl. Phys. **82**, 1236 (1997).
- ⁴¹S.-S. Li and J.-B. Xia, Phys. Lett. A **366**, 120 (2007).
- ⁴²S.-S. Li and J.-B. Xia, J. Appl. Phys. **101**, 093716 (2007).
- ⁴³S.-S. Li and J.-B. Xia, J. Appl. Phys. **100**, 083714 (2006).
- ⁴⁴Q.-R. Dong, S.-S. Li, Z.-C. Niu, S.-L. Feng, and H.-Z. Zheng, J. Appl. Phys. **96**, 3277 (2004).
- ⁴⁵J. M. Golden and B. I. Harpen, Phys. Rev. B **53**, 3893 (1996).
- ⁴⁶K. A. Matveev, L. I. Glazman, and H. U. Baranger, Phys. Rev. B **53**, 1034 (1996).
- ⁴⁷I. M. Ruzin, V. Chandrashekar, E. I. Levin, and L. I. Glazman, Phys. Rev. B **45**, 13469 (1992).
- ⁴⁸C. A. Stafford and S. Das Sharma, Phys. Rev. Lett. **72**, 3590 (1994).
- ⁴⁹G. Klimeck, G. Chen, and S. Datta, Phys. Rev. B **50**, 2316 (1994).
- ⁵⁰J. M. Golden and B. I. Harpen, Phys. Rev. B **53**, 3893 (1996).
- ⁵¹F. Troiani, U. Hohenester, and E. Molinari, Phys. Rev. B **65**, 161301 (2002).
- ⁵²B. Szafran, B. Stebe, and J. Adamowski, Phys. Rev. B **66**, 165331 (2002).
- ⁵³H. Imamura and P. A. Maksym, Phys. Rev. B **65**, 5817 (1998).
- ⁵⁴R. Ugajin, Phys. Rev. B **53**, 6963 (1995).
- ⁵⁵E. Paspalakis, Z. Kis, E. Voutsinas, and A. F. Terzis, Phys. Rev. B **69**, 155316 (2004).
- ⁵⁶G. Li, S. V. Branis, and K. K. Bajaj, Phys. Rev. B **47**, 15735 (1993).
- ⁵⁷H. C. Casey and M. B. Panesh, *Heterostructures Lasers, Part A* (Academic, New York, 1978).
- ⁵⁸S. V. Branis, G. Li, and K. K. Bajaj, Phys. Rev. B **47**, 1316 (1993).
- ⁵⁹A. M. Elabsy, Phys. Biol. **46**, 2621 (1992).
- ⁶⁰N. Raigoza, A. L. Morales, A. Monters, N. Porrás-Montenegro, and C. A. Duque, Phys. Rev. B **69**, 045323 (2004).
- ⁶¹D. B. T. Thoai, Physica B (Amsterdam) **175**, 373 (1991).